Eur. Phys. J. D **31**, 409–415 (2004)
DOI: 10.1140/epjd/e2004-00101-8

THE EUROPEAN PHYSICAL JOURNAL D

Emission spectrum for polar super rotors in a cold buffer gas

R.C. Forrey[a]

Penn State University, Berks-Lehigh Valley College, Reading PA 19610-6009, USA

Received 25 March 2004
Published online 10 August 2004 –

Abstract. Rate coefficients for cold and ultracold He+CO collisions are used together with radiative lifetimes to investigate the relaxation of rotationally hot polar molecules in the presence of a cold or ultracold helium buffer gas. Starting with an initial Gaussian distribution of highly excited rotational states, such as might be produced by an optical centrifuge, the time-dependent relaxation of a collection of super rotors is studied and in the case of CO an emission spectrum which contains the collisional information is predicted as a function of buffer gas density. Implications for the experimental detection of cold and ultracold quasiresonant atom-diatom scattering is discussed.

PACS. 33.20.-t Molecular spectra – 34.50.Ez Rotational and vibrational energy transfer

Forced molecular rotation using an optical centrifuge [1,2] or state-selective scheme [3] is a promising area of research that may provide a new direction in collision physics and chemistry. In particular, it is believed [3–6] that cold and ultracold temperatures would provide a rich context in which to study collisions with such highly excited "super rotors". Helium buffer gas cooling [7] has proven to be an effective technique for loading molecules into a magnetic trap [8] and it has recently been shown that the cooling technique may be applied to a beam of molecules [9]. An optical centrifuge [2] is capable of producing a beam of molecular super rotors. Therefore, it should be possible to direct such a beam into a buffer gas cell, or alternatively, to use the buffer gas to pre-cool the molecules before turning on the optical centrifuge. If the molecules possess an electric dipole moment, then the emission spectrum would contain a clear signature of the collisions and an opportunity to test fundamental phenomena such as the presence of quasiresonant vibration-rotation (QRVR) energy transfer. Atom-diatom collisions have been found to exhibit QR behavior at ordinary temperatures [10] and calculations have shown that QRVR energy transfer can occur at ultracold temperatures [4]. In fact, ultracold temperatures may provide the most interesting regime to study the QR effect in atom-diatom collisions. QR collisions are characterized by high efficiency and specificity. Time-dependent dynamical studies have shown [10] that the collisions proceed via a series of impulsive subcollisions that occur when the atom and diatom are collinear with the diatom near its outer vibrational turning point. As the translational temperature is decreased, the number of subcollisions increases. If the subcollisions add up in phase then a very efficient and specific transition will occur. This generally happens when the vibrational and rotational periods of the diatomic molecule are in resonance. Figure 1 shows some examples of resonant diatomic molecules. In each example, the vibrational period is related to the rotational period by an integer value. This allows retracing of the orbits of each atom. For homonuclear molecules, only even integer values are allowed and the atoms share the same orbit. Heteronuclear polar molecules can have odd integer matching of the vibrational and rotational periods. In this case, the orbits still retrace themselves, but each atom has its own orbit. Because of the retraced orbits, when a

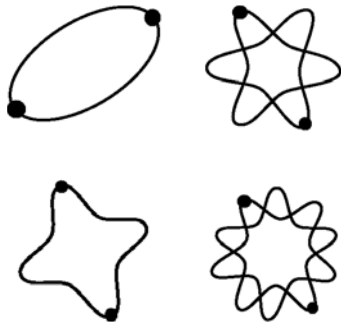

Fig. 1. Orbits of resonant vibrational and rotational motion for a diatomic molecule. The upper and lower left orbits correspond to $T_R = 2T_V$ and $T_R = 4T_V$, respectively, where T_R and T_V are the rotational and vibrational periods. The upper and lower right orbits correspond to $T_R = 3T_V$ and $T_R = 5T_V$, respectively. For the evenly matched periods on the left, each atom retraces a shared orbit. For the oddly matched periods on the right, each atom retraces its own separate orbit.

[a] e-mail: rcf6@psu.edu

resonant molecule interacts with an approaching atom, the subcollisions will add up in phase. The dominant transition will, therefore, follow a propensity rule [10] that is determined by the integer value of the matching diatomic periods. For example, the cases shown at the top of Figure 1 would have a propensity to undergo $\Delta j = -2\Delta v$ and $\Delta j = -3\Delta v$ transitions, respectively. If the molecule is not in resonance, the orbits do not retrace themselves and the subcollisions do not add in phase. Highly efficient and specific transitions can still occur, however, even when the orbits do not perfectly retrace themselves, an observation that led to the name quasiresonance [10]. Although QRVR transfer is not an energy resonant process, the initial rotational levels where the transitions typically take place may be estimated by looking at the energy gaps between the initial and final diatomic states. Figure 2 shows the energy gaps for CO($v = 1, j$) where v and j are the respective vibrational and rotational quantum numbers. The energy gaps for other vibrational levels are similar with the exception that the $v = 0$ plot would not include downward vibrational transitions. Our main interest in this kind of plot concerns the boxed regions where the energy gaps are small. In fact, at the crossing point the energy gap is positive and the QRVR transition is energetically not allowed. This differs from QRVR collisions at ordinary temperatures where the transitions can occur by borrowing energy from the translational motion. For cold and ultracold temperatures, however, there is very little translational energy in the collision and the energy gaps that are positive will remain closed. On either side of the crossing point, the energy gap becomes negative and the QRVR transition is energetically open. Therefore, there will be a very sharp jump in the total quenching rate coefficient as a function of initial rotational level. For $v = 0$, this jump will appear as a "step" at the j-value where the vibrationally upward QRVR transition becomes open. For $v > 0$, there will be jumps on either side of the j-values with positive energy gaps, and the distribution will appear to have a "hole" at these j-values. In the case of ultracold He+H_2 collisions, the jump in the total quenching rate coefficient for QRVR $\Delta j = -2\Delta v$ transitions is about 5 orders of magnitude [5]. For He+CO collisions, the jumps are typically a single order of magnitude or so [11], and the jumps are almost completely negligible for He+O_2 collisions [12].

The time-dependent relaxation of CO super rotors is investigated using the ultracold collision rate coefficients tabulated by Florian et al. [11]. The radiative lifetimes are obtained from the data of Chandra et al. [13] for $j \leq 140$ and from smooth extrapolations for $j > 140$. The kinetic rate equation is

$$\frac{d\,n_{vj}}{dt} = \sum_{v'j'} \left\{ \left(\tau^{-1}_{v'j'\to vj} + R_{v'j'\to vj}\,[\mathrm{He}] \right) n_{v'j'} - \left(\tau^{-1}_{vj\to v'j'} + R_{vj\to v'j'}\,[\mathrm{He}] \right) n_{vj} \right\} \quad (1)$$

where it is understood that the sums over v' and j' exclude v and j. This kinetic equation assumes that the positive source terms do not depend on translational energy. This will be a valid assumption if the elastic rate coefficients are much larger than all of the inelastic rate coefficients so that collision products are translationally cold immediately after an inelastic transition. The coupled states approximation used by Florian et al. [11] generally does not compute reliable elastic cross-sections, so it is difficult to confirm this assumption for He+CO. However, in the case of He+H_2 the elastic cross-sections for high-j strongly dominate the inelastic cross-sections for a wide range of translational energies [5]. Also, QRVR transitions are either suppressed at ultracold temperatures or else have small energy gaps that allow the collision products to remain translationally cold. Therefore, this kinetic model may still be a reasonable approximation even when the elastic collision rates are small. Equation (1) may be conveniently recast as a matrix equation

$$\frac{d\,n_m}{dt} = \sum_n M_{mn}\,n_n \quad (2)$$

with

$$M_{mn} = \tau^{-1}_{v'j'\to vj} + R_{v'j'\to vj}\,[\mathrm{He}] \quad (3)$$

and

$$M_{mm} = -\sum_{v'j'} \left(\tau^{-1}_{vj\to v'j'} + R_{vj\to v'j'}\,[\mathrm{He}] \right). \quad (4)$$

Figures 3–6 show the solution to equation (2) assuming an initial Gaussian distribution of CO molecules centered at $j = 180$ with $v = 0$. A constant buffer gas density of 10^{15} cm^{-3} was used for each of the calculations. After 5 ms, the $v = 0$ distribution has decreased in density and shifted downward in j. The loss of density for $v = 0$ is due

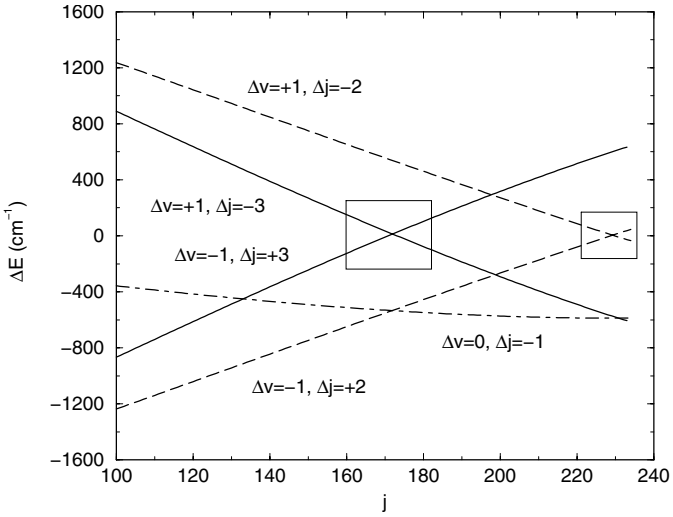

Fig. 2. Energy gaps between initial and final ro-vibrational states for CO. The boxed regions show where QRVR transitions typically occur. In both cases, the energy gap is positive at the crossing point between the two curves. Interesting threshold behavior may be expected for cold collisions near these j-values.

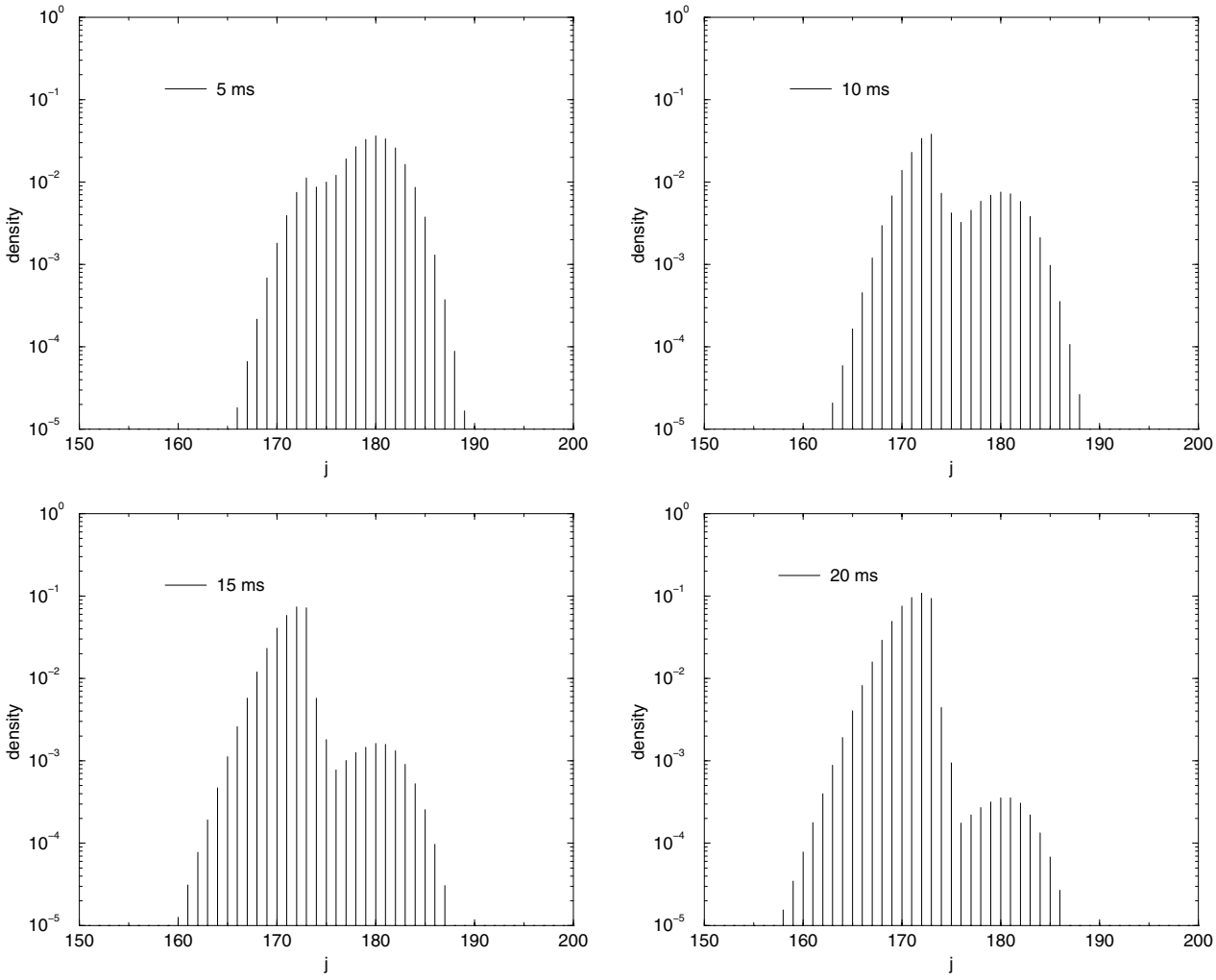

Fig. 3. Density of CO($v = 0, j$) as a function of time. The frames are separated by 5 ms following an initial Gaussian distribution centered about $j = 180$ with $v = 0$. The buffer gas density is 10^{15} cm^{-3} and the CO density is normalized to unity.

to transitions to the $v > 0$ levels (see Figs. 4–6) which were initially unpopulated. After 10 ms, the $v = 0$ distribution has continued to shift downward with a peak emerging at $j = 173$. This is the same location as the "step" in the zero-temperature rate coefficient distribution [11]. For $v > 0$, the peaks in the densities for $j = 170{-}173$ begin to become more prominent. These values of j are the same locations as the "holes" in the distribution of rate coefficients [11]. The interpretation of this time evolution is becoming clear: the initial $v = 0$ distribution of super rotors redistribute via $\Delta j = -3\Delta v$ transitions which are quasiresonant. At a step or hole location where the QR transition is energetically unavailable, the total quenching rate coefficient is greatly suppressed and the densities of super rotors begin to peak. After 15 or 20 ms, the peaks are even more prominent and the density at $j \approx 180$ has dropped by 2−3 orders of magnitude. The population of vibrationally excited states occurs only through a rapid succession of very specific and efficient $\Delta v = +1, \Delta j = -3$ transitions. These transitions move a significant density of molecules all the way up the vibrational ladder, particularly when the buffer gas density is large. For time steps that are greater than about 20 ms, the densities begin to gradually move downward in both v and j as a result of pure rotational collisional transitions, vibrationally downward QRVR transitions, and radiative decay. If the buffer gas density is increased, then this time scale would be shorter, however, the overall behavior would be very similar. Also, if the initial distribution of super rotors was centered about a different j-value, then the time-dependence would follow a path that is controlled by the nearest set of QRVR steps and holes [11].

The time-dependent densities may be integrated to produce an emission spectrum. The intensity of the emission spectrum is given by

$$I_{vj\to v'j'} = \tau^{-1}_{vj\to v'j'} \int n_{vj}(t)\, dt \tag{5}$$

where $v' = v - 1$ with $j' = j + 1$ for the P-branch and $j' = j - 1$ for the R-branch spectrum. Because n_{vj}

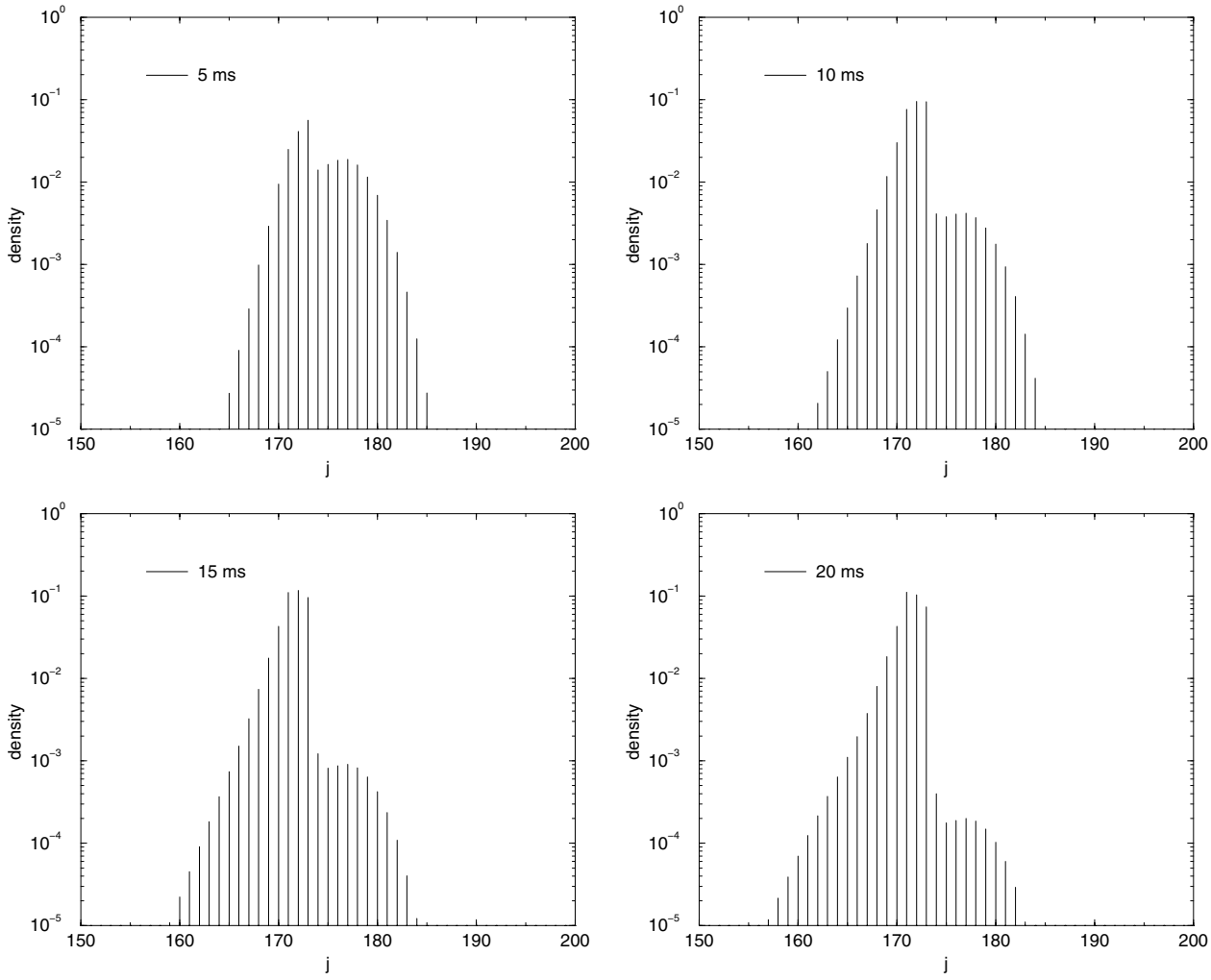

Fig. 4. Density of CO($v = 1, j$) as a function of time. The frames are separated by 5 ms following an initial Gaussian distribution centered about $j = 180$ with $v = 0$. The buffer gas density is 10^{15} cm^{-3} and the CO density is normalized to unity. The initially unpopulated $v = 1$ manifold is rapidly populated due to the efficiency of $\Delta v = +1, \Delta j = -3$ transitions.

represents the fraction of CO molecules that are in the state (v, j), the spectral intensity in equation (5) is normalized to a single CO molecule. Figures 7 and 8 show the intensity versus wavelength spectrum that would be produced by the experimental conditions described above. The R-branch spectrum shows several sets of lines separated by ∼50 nm. Each set of lines was produced by a different vibrational level as indicated in the figure. The number of lines in each set is equal to the number of rotational levels contained in each "hole" in the distribution of rate coefficients. For a buffer gas density of 10^{15} cm^{-3}, the contributions from $v > 5$ are negligible. Spectral lines from higher vibrational levels would be obtained using a larger buffer gas density. In fact, it should be possible to obtain spectral lines corresponding to vibrational levels going all the way to dissociation by simply increasing the buffer gas density and using shorter integration times. The P-branch spectrum also shows a characteristic set of lines that could be used to analyze the collisions. The contributions from the various vibrational levels are not as well-separated, however, and the spectrum appears more congested than the associated R-branch spectrum.

Figures 3–8 were obtained using rate coefficients that were computed in the limit of zero temperature [11]. As the temperature is increased, the structure in the rate coefficient distributions will eventually disappear as the closed QRVR transitions become energetically accessible. A temperature-dependent study of He+CO rate coefficients [11] showed that the hole in the $v = 1$ distribution at $j = 171-173$ disappeared for temperatures greater than 30 K but remained prominent for temperatures as large as 300−500 mK. This is the same temperature range as the buffer gas cooling experiments of Doyle and co-workers [7–9]. Therefore, the emission spectrum predicted in Figures 7 and 8 would be nearly identical to one obtained at 300−500 mK and could be achieved using a standard buffer gas setup [7] without the need for magnetic trapping [8]. An optical centrifuge [1,2] has the

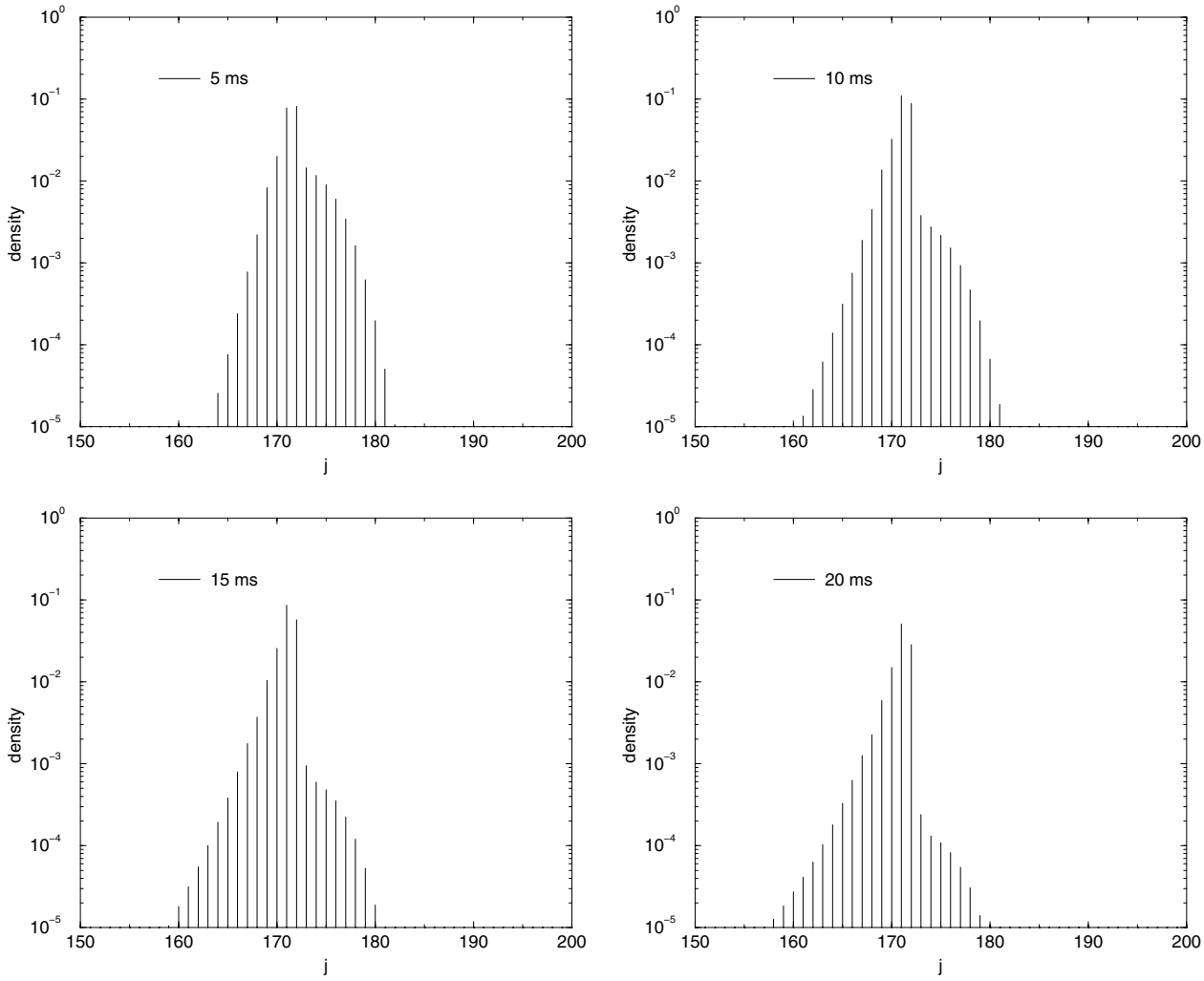

Fig. 5. Density of CO($v = 2, j$) as a function of time. The frames are separated by 5 ms following an initial Gaussian distribution centered about $j = 180$ with $v = 0$. The buffer gas density is 10^{15} cm^{-3} and the CO density is normalized to unity. The initially unpopulated $v = 2$ manifold is rapidly populated due to the efficiency of $\Delta v = +1, \Delta j = -3$ transitions.

capability to produce an initial distribution of molecular super rotors. By centering this distribution near an energy gap crossing point (see Fig. 2) it should be possible to obtain an emission spectrum that is characteristic of each of the QRVR propensity rules. For example, the initial distribution about $j = 180$ that was assumed in the present calculations produces a spectrum that is characteristic of QRVR $\Delta j = -3\Delta v$ transitions. A similar study using an initial distribution centered around $j = 230$ would produce a spectrum that is characteristic of QRVR $\Delta j = -2\Delta v$ transitions. Initial distributions that include vibrational excitation would introduce additional opportunities for studying cold or ultracold QRVR transitions.

Cold or ultracold collisions involving molecular super rotors is an interesting subject in that it combines quantum mechanical translational motion with nearly classical rotational motion. A qualitative correspondence between fully quantal and fully classical QR behavior has been demonstrated theoretically [4] and it is hoped that QRVR energy transfer in a cold or ultracold atom-diatom collision would soon be investigated experimentally. Polar molecules such as CO offer an opportunity to perform such investigations due to the signal arising from the radiating electric dipole moment. At low translational temperatures, the rotational distribution of total collisional quenching rate coefficients contains sharp structure due to the presence or absence of QRVR transitions. This structure would exert a strong influence on the emission spectrum, and therefore, an experimental measure of the QRVR phenomena at cold or ultracold temperatures.

This work was supported by NSF Grant No. PHY-0244066.

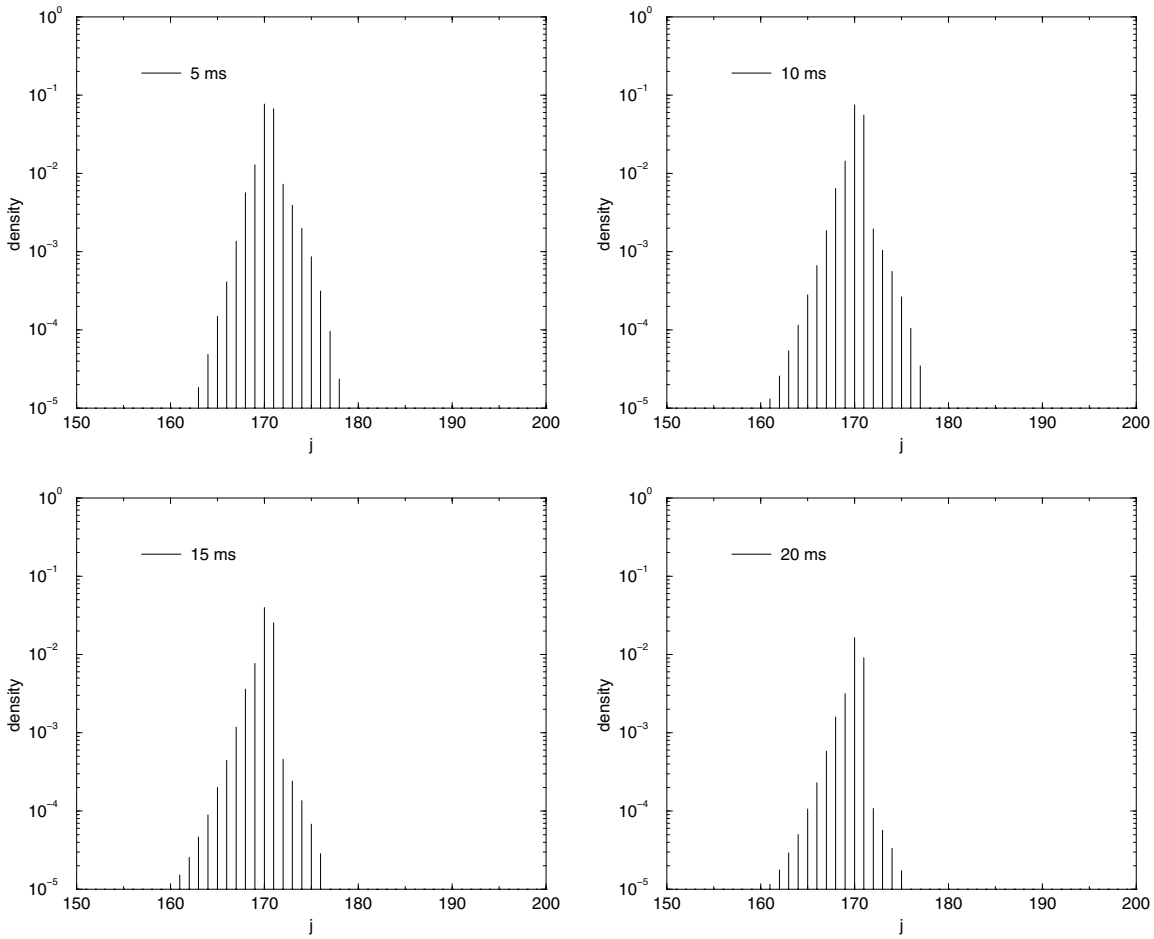

Fig. 6. Density of CO($v = 3, j$) as a function of time. The frames are separated by 5 ms following an initial Gaussian distribution centered about $j = 180$ with $v = 0$. The buffer gas density is 10^{15} cm^{-3} and the CO density is normalized to unity. The initially unpopulated $v = 3$ manifold is rapidly populated due to the efficiency of $\Delta v = +1, \Delta j = -3$ transitions.

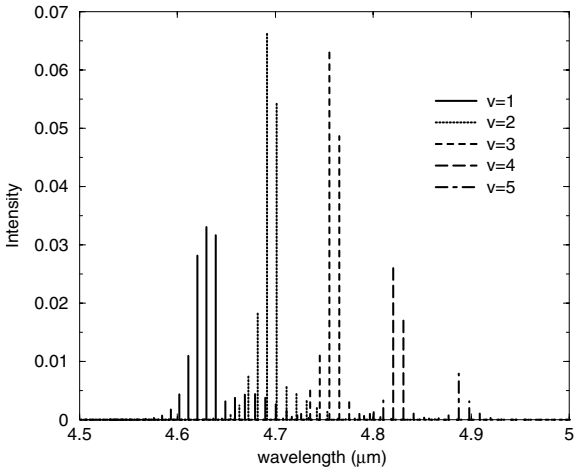

Fig. 7. R-branch emission spectrum produced by an initial Gaussian distribution of CO molecules centered at $j = 180$ and $v = 0$ with a helium buffer gas density of 10^{15} cm^{-3}. The excited vibrational levels are populated by QRVR collisions and the associated radiative decay from each level is indicated in the figure.

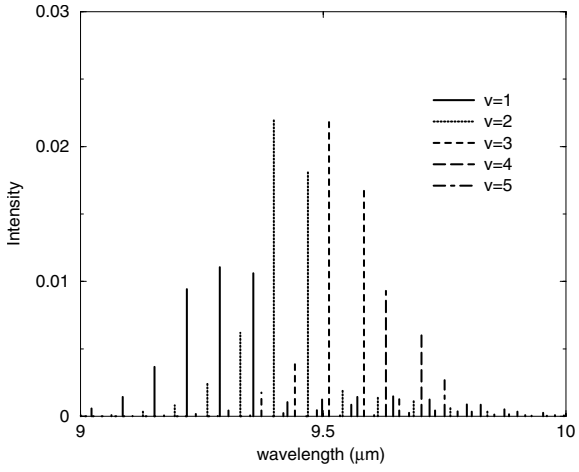

Fig. 8. P-branch emission spectrum produced by an initial Gaussian distribution of CO molecules centered at $j = 180$ and $v = 0$ with a helium buffer gas density of 10^{15} cm^{-3}. The excited vibrational levels are populated by QRVR collisions and the associated radiative decay from each level is indicated in the figure.

References

1. J. Karczmarek, J. Wright, P. Corkum, M. Ivanov, Phys. Rev. Lett. **82**, 3420 (1999)
2. D.M. Villeneuve, S.A. Aseyev, P. Dietrich, M. Spanner, M.Y. Ivanov, P.B. Corkum, Phys. Rev. Lett. **85**, 542 (2000)
3. J. Li, J.T. Bahns, W.C. Stwalley, J. Chem. Phys. **112**, 6255 (2000)
4. R.C. Forrey, N. Balakrishnan, A. Dalgarno, M. Haggerty, E.J. Heller, Phys. Rev. Lett. **82**, 2657 (1999); R.C. Forrey, N. Balakrishnan, A. Dalgarno, M. Haggerty, E.J. Heller, Phys. Rev. A **64**, 022706 (2001)
5. R.C. Forrey, Phys. Rev. A **63**, 051403 (2001); R.C. Forrey, Phys. Rev. A **66**, 023411 (2002)
6. A.J. McCaffery, J. Chem. Phys. **113**, 10947 (2000)
7. J.M. Doyle, B. Friedrich, J. Kim, D. Patterson, Phys. Rev. A **52**, R2515 (1995)
8. J.D. Weinstein, R. deCarvalho, T. Guillet, B. Friedrich, J.M. Doyle, Nature **395**, 148 (1998)
9. D. Egorov, T. Lahaye, W. Schollkopf, B. Friedrich, J.M. Doyle, Phys. Rev. A **66**, 043401 (2002)
10. B. Stewart, P.D. Magill, T.P. Scott, J. Derouard, D.E. Pritchard, Phys. Rev. Lett. **60**, 282 (1988); P.D. Magill, B. Stewart, N. Smith, D.E. Pritchard, Phys. Rev. Lett. **60**, 1943 (1988)
11. P. Florian, M. Hoster, R.C. Forrey, Phys. Rev. A **70**, 032709 (2004)
12. K. Tilford, M. Hoster, P. Florian, R.C. Forrey, Phys. Rev. A **69**, 052705 (2004)
13. S. Chandra, V.U. Maheshwari, A.K. Sharma, Astron. Astrophys. Suppl. Ser. **117**, 557 (1996); extensive tables at `http://vizier.u-strasbg.fr/viz-bin/VizieR`